© 2016. Published by The Company of Biologists Ltd | Development (2016) 143, 2089-2102 doi:10.1242/dev.131995

The EGFR signaling pathway controls gut progenitor differentiation during planarian regeneration and homeostasis

Sara Barberán, Susanna Fraguas and Francesc Cebrià*

ABSTRACT

The planarian *Schmidtea mediterranea* maintains and regenerates all its adult tissues through the proliferation and differentiation of a single population of pluripotent adult stem cells (ASCs) called neoblasts. Despite recent advances, the mechanisms regulating ASC differentiation into mature cell types are poorly understood. Here, we show that silencing of the planarian EGF receptor *egfr-1* by RNA interference (RNAi) impairs gut progenitor differentiation into mature cells, compromising gut regeneration and maintenance. We identify a new putative EGF ligand, *nrg-1*, the silencing of which phenocopies the defects observed in *egfr-1(RNAi)* animals. These findings indicate that *egfr-1* and *nrg-1* promote gut progenitor differentiation, and are thus essential for normal cell turnover and regeneration in the planarian gut. Our study demonstrates that the EGFR signaling pathway is an important regulator of ASC differentiation in planarians.

KEY WORDS: Planarian, *Schmidtea mediterranea*, Epidermal growth factor receptor, Differentiation, Tissue turnover, Stem cell

INTRODUCTION

Adult stem cells (ASCs) usually mediate the normal turnover of adult tissues and their repair after injury. The balance between ASC proliferation and differentiation needs to be tightly regulated because any alteration can lead to depletion or overgrowth of the ASC population, resulting in premature aging or cancer (Oh et al., 2014; Visvader, 2011). The decision to either self-renew or differentiate is controlled by intrinsic determinants present in ASCs and/or extrinsic signals from neighboring differentiated tissues (Morrison and Spradling, 2008). However, a comprehensive understanding of the exact molecular mechanisms controlling ASC maintenance and differentiation is lacking.

Freshwater planarians constitute an attractive model for the *in vivo* study of stem cell biology in homeostatic and regenerating conditions (Gentile et al., 2011; Newmark and Sánchez Alvarado, 2002; Rink, 2013). These organisms have an impressive capacity to regenerate missing body parts (Morgan, 1898; Reddien and Sánchez Alvarado, 2004), and to grow or degrow depending on environmental conditions (Baguña, 2012; Oviedo et al., 2003; Pellettieri et al., 2010; Romero and Baguña, 1991). These unique abilities arise from a population of pluripotent ASCs, the so-called neoblasts (Baguña et al., 1989; Reddien and Sánchez Alvarado, 2004; Rink, 2013; Wagner et al., 2011). Neoblasts are the only dividing cells of planarians (Morita and Best, 1984; Newmark and Sánchez Alvarado, 2000) and thus can differentiate into any cell type. Accordingly, the neoblast population consists of a compartment of pluripotent ASCs (Wagner et al., 2011) and a heterogeneous pool of lineage-restricted progenitors (Hayashi et al., 2010; Moritz et al., 2012; Reddien, 2013; Scimone et al., 2014; van Wolfswinkel et al., 2014), which can be distinguished by the expression of tissue-specific transcription factors (Adler et al., 2014; Cowles et al., 2013; Lapan and Reddien, 2012; Scimone et al., 2014, 2011; Wagner et al., 2011). Despite recent advances, the genes and molecular pathways that regulate the differentiation of known progenitors into distinct mature cell types remain poorly understood.

The epidermal growth factor receptor (EGFR) pathway is implicated in numerous biological processes (Cela and Llimargas, 2006; Jiang and Wu, 2014; Lyons et al., 2005) and is commonly involved in stem cell proliferation, maintenance and differentiation (Aguirre et al., 2010; Aroian et al., 1990; Biteau and Jasper, 2011; Li et al., 2015). In the planarian *Schmidtea mediterranea*, one putative EGF ligand (*epiregulin-1*) (Wenemoser et al., 2012) and four EGF receptors (*egfr-1*, *egfr-2*, *egfr-3* and *egfr-5*) (Fraguas et al., 2011; Rink et al., 2011) have been identified to date. Although no function has yet been attributed to *epiregulin-1* or *egfr-2*, the receptors *egfr-1*, *egfr-3* and *egfr*-5 are required for regeneration and maintenance of various planarian tissues. However, the exact role of the EGFR pathway in neoblast biology is still unclear.

Here, we demonstrate that EGFR signaling controls the differentiation of gut progenitors, and hence the regeneration and homeostasis of the planarian intestine. We show that *egfr-1 (RNAi)* animals are unable to regenerate and maintain the normal morphology of the gut. The loss of gastrodermis is not due to increased apoptosis within this tissue, but to impaired differentiation of gut progenitors into mature gastrodermal cells. Moreover, we identify a new putative EGF ligand, *nrg-1*, which is expressed in the mesenchyme and pharynx. Silencing of *nrg-1* phenocopies the defects caused by *egfr-1* RNAi, suggesting that *nrg-1*-mediated signaling might induce the differentiation of gut progenitors via *egfr-1*. Our findings support a conserved role of EGFR signaling in controlling the differentiation and overall stability of neoblasts.

RESULTS

egfr-1 is required for gut regeneration

Consistent with previous studies (Fraguas et al., 2011), fluorescent *in situ* hybridization of *egfr-1* (Fig. 1A) revealed expression in the eye pigment cells (Fig. 1Aa), pharynx and mouth opening (Fig. 1Ab), and gut (Fig. 1Ac), and in discrete cells within the mesenchyme (Fig. 1Ac). The colocalization of *egfr-1* and SMEDWI-1, a specific neoblast marker (Guo et al., 2006; Marz et al., 2013), indicated that *egfr-1* is expressed in neoblasts and/or immediate neoblast descendants (Fig. 1B).

Department of Genetics, Faculty of Biology, University of Barcelona and Institute of Biomedicine of the University of Barcelona (IBUB), Av. Diagonal 643, Edifici Prevosti, Planta 1, Barcelona, Catalunya 08028, Spain.

*Author for correspondence (fcebrias@ub.edu)

F.C., 0000-0002-4028-3135

Received 15 October 2015; Accepted 12 April 2016

Development (2016) 143, 2089-2102 doi:10.1242/dev.131995

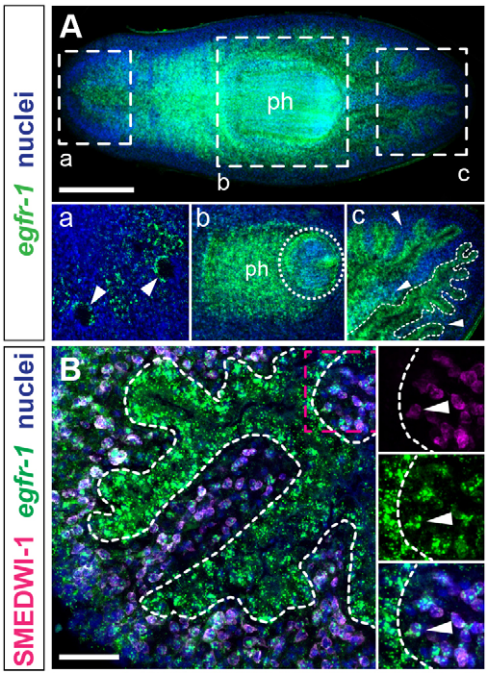

Fig. 1. *egfr-1* expression pattern. (A) Whole-mount fluorescent *in situ* hybridization of *egfr-1*. Boxed regions a-c are magnified beneath. *egfr-1* expression in: eye pigment cells (a, arrowheads), pharynx and mouth (b, dashed circle), gut (c, delimited with a dashed line) and in discrete mesenchymal cells (c, arrowheads). (B) Overlay of *egfr-1* expression with that of the neoblast marker SMEDWI-1. The boxed region is magnified on the right to show colocalization of *egfr-1* and SMEDWI-1 (white arrowheads). Dashed lines demarcate the gut. In all panels, nuclei are counterstained with TO-PRO-3. A shows ventral view with anterior end oriented to the left. ph, pharynx. Scale bars: 250 µm in A; 50 µm in B.

The planarian intestine is composed of one anterior and two posterior main gut branches, which ramify into secondary, tertiary and quaternary branches (Fig. 2A) (Forsthoefel et al., 2011). We used the specific marker *panthotenate kinase 1* (*pk-1*) (Fraguas et al., 2014) to examine gut morphology during regeneration after *egfr-1* RNAi (Fig. 2B-S). During posterior regeneration in head fragments (Fig. 2B-G), control animals developed new intestinal branches, which projected around the newly formed pharynx after 1 week (Fig. 2B). In *egfr-1(RNAi)* animals, these regenerating branches were shorter and failed to completely enclose the pharynx (Fig. 2C). After 2 weeks, the new posterior primary branches extended towards the posterior end and began to produce secondary branches in controls (Fig. 2D). By contrast, the new posterior primary branches in *egfr-1(RNAi)* animals did not elongate and failed to produce secondary branches (Fig. 2E). After 3 weeks, new secondary and tertiary gut branches were observed in controls (Fig. 2F), but not in *egfr-1(RNAi)* animals (Fig. 2G).

In regenerating trunk pieces (Fig. 2H-M), elongation of the pre-existing anterior and posterior primary branches within the blastema was observed after 1 week of regeneration in controls (Fig. 2H,H′). After 2 weeks, new primary branches ramified to form secondary and tertiary gut branches (Fig. 2J,J′), restoring the original pattern 3 weeks after amputation (Fig. 2L,L′). Although elongation of the pre-existing primary branches was also observed in *egfr-1(RNAi)* animals (Fig. 2I,I′), no new secondary or tertiary branches were formed (Fig. 2K,K′), and these animals ultimately failed to regenerate a normal gut (Fig. 2M,M′).

In regenerating tail fragments (Fig. 2N-S), the pre-existing posterior branches converged and fused in the midline to form the new anterior branch 1 week after amputation in controls (Fig. 2N). While this event was also observed in *egfr-1(RNAi)* animals, the new anterior branch was shorter (Fig. 2O). After 2 weeks, secondary branches began to develop in controls (Fig. 2P), but were almost absent in most *egfr-1(RNAi)* animals (Fig. 2Q). Finally, after 3 weeks, the normal gut pattern had been restored in controls (Fig. 2R), whereas *egfr-1(RNAi)* animals had failed to regenerate nearly any secondary or tertiary branches (Fig. 2S).

Remarkably, all *egfr-1(RNAi)* animals analyzed lost almost all secondary and tertiary branches of the pre-existing gut (Fig. 2G,M,S). Similarly, in line with previous results (Fraguas et al., 2011), all *egfr-1(RNAi)* animals showed defects in pharynx regeneration (Fig. 2G,S), exhibiting a reduced pharynx cavity compared with control animals (Fig. 2F,R). Taken together, these results indicate that *egfr-1* is necessary for proper regeneration of the planarian digestive system, and suggest a possible role of this gene in the maintenance thereof.

egfr-1 is required for the maintenance of gut morphology

We next examined the morphology of the gut in intact control and *egfr-1(RNAi)* animals (Fig. 3). Two weeks after the final *egfr-1* dsRNA injection, both control and *egfr-1(RNAi)* animals showed the typical gut morphology (Fig. 3A,E). However, after 4 weeks, *egfr-1(RNAi)* animals differed from controls in that they exhibited a less ramified gut, with fewer tertiary and quaternary branches (Fig. 3B,F). Moreover, the gut branches of *egfr-1(RNAi)* animals were thinner than those of controls (Fig. 3Bb,Fb). By 6 weeks, *egfr-1(RNAi)* animals showed more severe defects: few tertiary and almost no quaternary branches remained in these animals, in contrast to controls, in which both branches were maintained (Fig. 3C,G). The most extreme phenotype was observed 8 weeks after RNAi: *egfr-1(RNAi)* animals had completely lost all tertiary and quaternary branches, with only some secondary branches remaining (Fig. 3H). At this time point, the anterior primary branch, and to a lesser extent the posterior primary branches, were shorter in *egfr-1(RNAi)* animals compared with controls (Fig. 3D,H). As seen during regeneration, *egfr-1(RNAi)* animals already exhibited a wider and thicker pharyngeal cavity 4 weeks after treatment (Fig. 3B,F).

To better understand the progression of the *egfr-1* RNAi phenotype during homeostasis, we quantified the length of the primary gut branches and the number of secondary, tertiary and quaternary branches (Fig. 3I). Although the effect was less severe in the posterior region, from 4 weeks onwards both the anterior and posterior primary gut branches were significantly shorter in *egfr-1 (RNAi)* animals compared with controls (Fig. 3J). By 2 weeks, a significant reduction in the number of quaternary branches in the anterior region was also observed, followed by a decrease in the numbers of tertiary and secondary branches by 4 and 8 weeks, respectively (Fig. 3K). In the posterior region the dynamics of the phenotype were similar to those of the anterior region, albeit with a slight delay (Fig. 3L). Overall, quantitative analysis of the number and length of gut branches in *egfr-1(RNAi)* animals indicated that the disappearance of the branches occurred in a stereotypical, organized fashion (Fig. 3J-L), sequentially affecting the quaternary, tertiary and finally secondary branches, accompanied by progressive shortening of the primary branch. Our data thus indicate that while control animals were capable of maintaining their gut morphology over time, *egfr-1(RNAi)* animals were unable to preserve the integrity of the gut, as evidenced by the gradual shortening of this structure and the loss of gut branches.

Development (2016) 143, 2089-2102 doi:10.1242/dev.131995

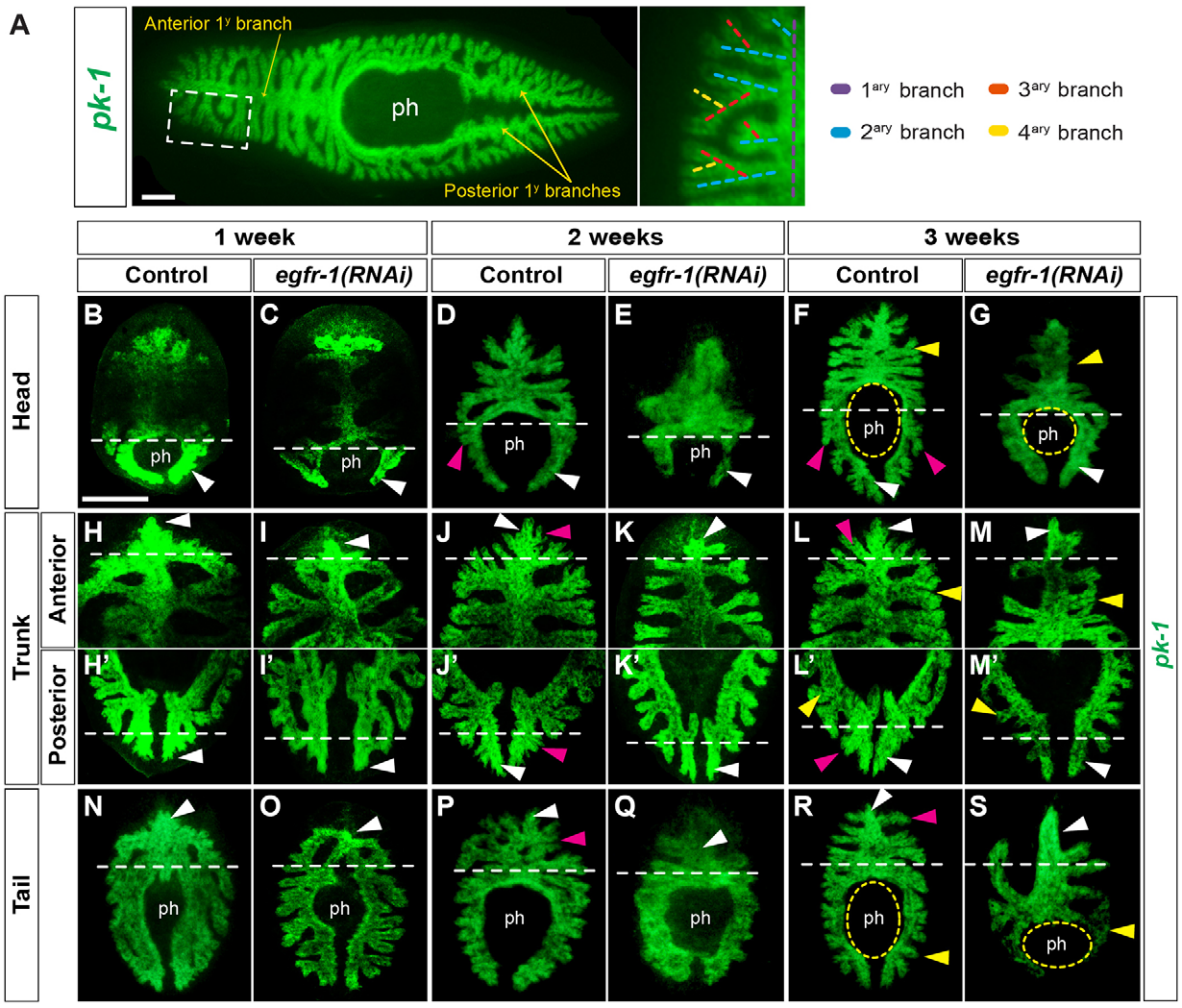

Fig. 2. Gut regeneration defects in *egfr-1(RNAi)* animals. (A) Normal gut morphology visualized with *pk-1*. Whole-mount fluorescent *in situ* hybridizations with *pk-1* in regenerating head fragments (B-G), anterior (H-M) and posterior (H′-M′) bipolar trunk fragments, and tail fragments (N-S). Regeneration time is indicated on top. *egfr-1(RNAi)* animals show abnormal growth of new primary branches (white arrowheads) and fail to regenerate secondary and tertiary branches (magenta arrowheads). *egfr-1(RNAi)* animals lose the pre-existing branches (yellow arrowheads) and display pharynx defects (yellow circles). Dashed horizontal lines roughly separate regenerated from pre-existing tissue. The anterior end is oriented to the left in A, and to top in all other images. ph, pharynx. Scale bars: 250 µm in A,B (applies to B-S).

egfr-1 silencing affects gastrodermis integrity

The planarian gastrodermis is a monostratified epithelium composed of two cell types, absorptive phagocytes and secretory goblet cells, surrounded by an enteric muscular plexus (Bowen et al., 1974; Bueno et al., 1997; Kobayashi et al., 1998). To better characterize the loss of the gut after *egfr-1* RNAi, we performed a detailed histological analysis of the gastrodermis. Specifically, we studied intact *egfr-1 (RNAi)* animals that were fixed 4 weeks after the last RNAi injection, the earliest time point at which all the features of the *egfr-1* phenotype were evident (Fig. 3). As observed in representative transverse sections corresponding to four different positions along the antero-posterior axis of the planarian body, *egfr-1(RNAi)* animals had fewer and smaller gut diverticula per section than controls (Fig. 4A). Importantly, the defects in the gastrodermis in *egfr-1(RNAi)* animals were not correlated with loss of the enteric musculature surrounding the diverticula (anti-MHC) (Cebrià et al., 1997), which appeared to be unaffected (Fig. 4A). Moreover, Mallory's staining in sagittal sections revealed a reduced and aberrant gastrodermis in *egfr-1 (RNAi)* animals, without the characteristic columnar disposition of cells evident in control animals (Fig. 4B).

To support our qualitative observations, we performed quantitative analyses of the area of the gastrodermis in anterior and posterior sections of control and *egfr-1(RNAi)* animals (Fig. 4C). Consistently, *egfr-1* RNAi resulted in a significant decrease in the gastrodermal area in both regions (Fig. 4D). Quantification of the number of nuclei per diverticulum showed that the gastrodermis of *egfr-1(RNAi)* animals contained fewer nuclei than that of controls. However the number of nuclei relative to the area of the diverticulum remained constant, as this area was also significantly reduced in *egfr-1(RNAi)* animals (Fig. 4E). To determine whether cell loss affected one or both gastrodermal cell types, we used an anti-RPZ-1 antibody to specifically label goblet cells (Reuter et al., 2015) (Fig. 4F). Immunostaining of anterior and posterior sections revealed a significant reduction in the number of goblet cells in *egfr-1(RNAi)* animals compared with controls (Fig. 4F,G). As observed with Mallory's staining, the goblet cells of *egfr-1(RNAi)* animals showed abnormal morphologies (Fig. 4F). We estimated the number of phagocytes by subtracting the number of goblet cells from the total number of gastrodermal cells as identified using the nuclear marker DAPI. The gastrodermis of *egfr-1(RNAi)* animals contained fewer phagocytes than that of controls, although the

Development (2016) 143, 2089-2102 doi:10.1242/dev.131995

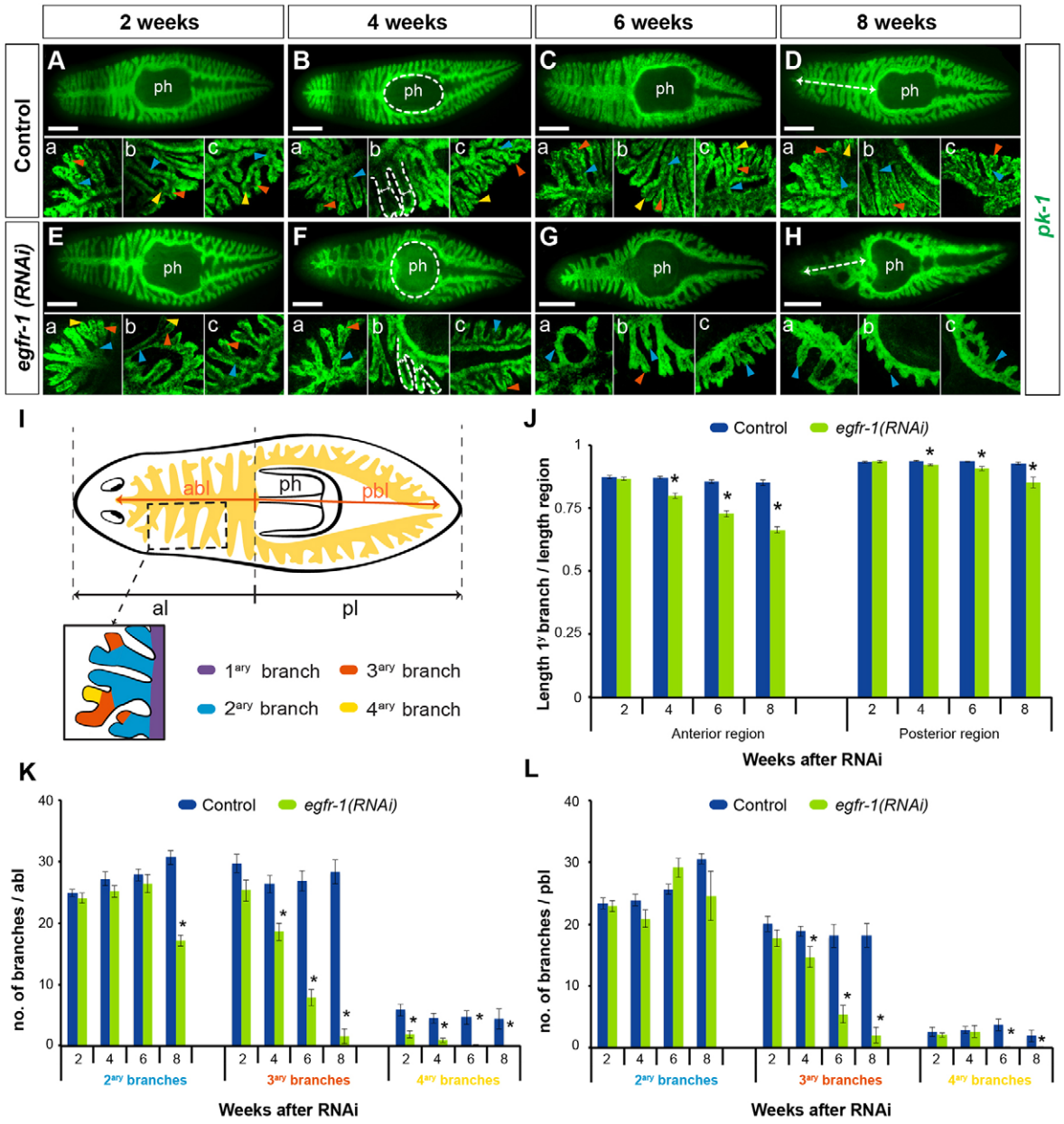

Fig. 3. Gut homeostasis defects in *egfr-1(RNAi)* animals. (A-H) Whole-mount fluorescent *in situ* hybridization with *pk-1*. Time since the last RNAi injection is indicated on top. (A-D) Maintenance of the typical gut morphology in controls. (E-H) *egfr-1(RNAi)* animals show a gradual loss of quaternary, tertiary and secondary branches (yellow, red and blue arrowheads, respectively). Details of each region are shown in panels a-c below. A marked narrowing of the branches (arrows in Bb,Fb), a shortening of the primary branch (arrows in D,H) and defects in the morphology of the pharynx cavity (white circles) are evident. (I) Methodology used for the quantitative analyses of *egfr-1(RNAi)* phenotype. (J) Shortening of the anterior and posterior primary branches in *egfr-1(RNAi)* animals. (K,L) Reduction in the number of branches in the anterior (K) and posterior (L) regions in *egfr-1(RNAi)* animals. In all statistical analyses n=10 and error bars represent s.e.m. *P<0.05 (Student's t-test). In all panels the anterior end is oriented to the left. ph, pharynx; abl, anterior branch length; pbl, posterior branch length; al, anterior region length; pl, posterior region length. Scale bars: 250 µm.

number of phagocytes relative to the area of the diverticulum remained constant in both control and *egfr-1(RNAi)* animals (Fig. 4H). Together, these results indicate that the morphological defects observed in *egfr-1(RNAi)* animals involve a reduction in gastrodermis area and depletion of both gastrodermal cell types.

Impaired gut progenitor cell differentiation accounts for the loss of gastrodermis in *egfr-1(RNAi)* animals

To determine whether the decrease in the number of cells in the gastrodermis of *egfr-1(RNAi)* animals was due to increased apoptosis, we performed TUNEL assays to quantify apoptotic cells (Pellettieri et al., 2010) in transverse sections of intact animals after *egfr-1* RNAi (Fig. 5A). *egfr-1* RNAi resulted in a significant increase in the number of apoptotic mesenchymal cells (Fig. 5B). However, there were no significant differences in the number of apoptotic gastrodermal cells between control and *egfr-1(RNAi)* animals (Fig. 5C), suggesting that the decrease in cell number seen in RNAi animals was not caused by an abnormal increase in apoptosis within this tissue.

We next investigated whether impaired differentiation of new cells could explain the defects seen after *egfr-1* RNAi. To test this

Development (2016) 143, 2089-2102 doi:10.1242/dev.131995

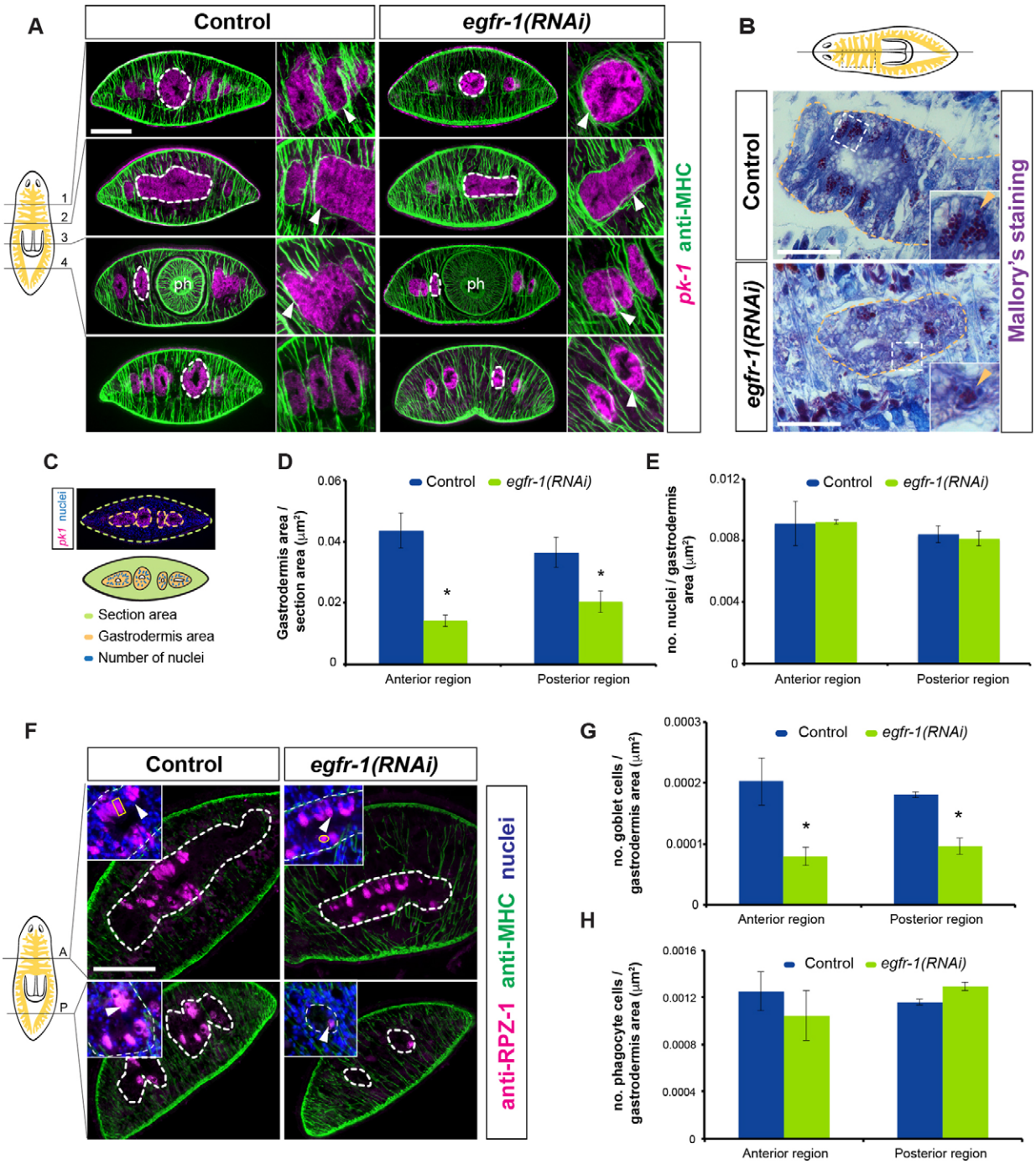

Fig. 4. Reduction in the area of the gastrodermis and loss of gut cells in *egfr-1(RNAi)* animals. (A) Fluorescent *in situ* hybridization with *pk-1* combined with immunohistochemistry with anti-MHC in transverse sections. Magnified images are shown on the right-hand side. *egfr-1(RNAi)* animals have fewer diverticula and a smaller gastrodermis area (dashed circles), but show no muscular defects (white arrowheads). (B) Mallory's staining of gastrodermal tissue in sagittal sections. *egfr-1(RNAi)* animals show a reduced and abnormal gastrodermis (yellow dashed lines; high-magnifications on the right show details of the cellular morphology, yellow arrowheads indicate secretory granules). (C) Methodology used to quantitatively assess the defects in *egfr-1(RNAi)* animals. (D,E) Quantification of the gastrodermis area (D) and the number of gastrodermal cells (E) in control and *egfr-1(RNAi)* animals. (F) Immunohistochemistry with goblet cell-specific antibody (anti-RPZ-1; magenta) in transverse sections, combined with anti-MHC and DAPI counterstaining (dashed lines delimit the gastrodermis). Magnifications within the panels show the reduced number (white arrowheads) and aberrant shape (enclosed with yellow line) of the goblet cells in *egfr-1(RNAi)* animals. (G,H) Quantification of the number of goblet cells (G) and phagocytes (H) in control and *egfr-1(RNAi)* animals. In all statistical analyses $n=5$ animals, with 2-5 sections per animal and position analyzed. Error bars represent s.e.m. $^*P<0.05$ (Student's *t*-test). In all sections, the dorsal aspect is oriented towards the top. ph, pharynx. Scale bars: 100 µm in A,F; 50 µm in B.

hypothesis we labeled S-phase neoblasts using the thymidine analog F-ara-EdU in control and *egfr-1(RNAi)* animals (Zhu et al., 2015). After a 6-day chase, the presence of EdU-labeled cells was assessed in histological sections (Fig. 5D). While control animals showed EdU-labeled cells within the gastrodermis, almost no EdU incorporation was observed in the gut tissue of *egfr-1(RNAi)* animals (Fig. 5D,E).

Development (2016) 143, 2089-2102 doi:10.1242/dev.131995

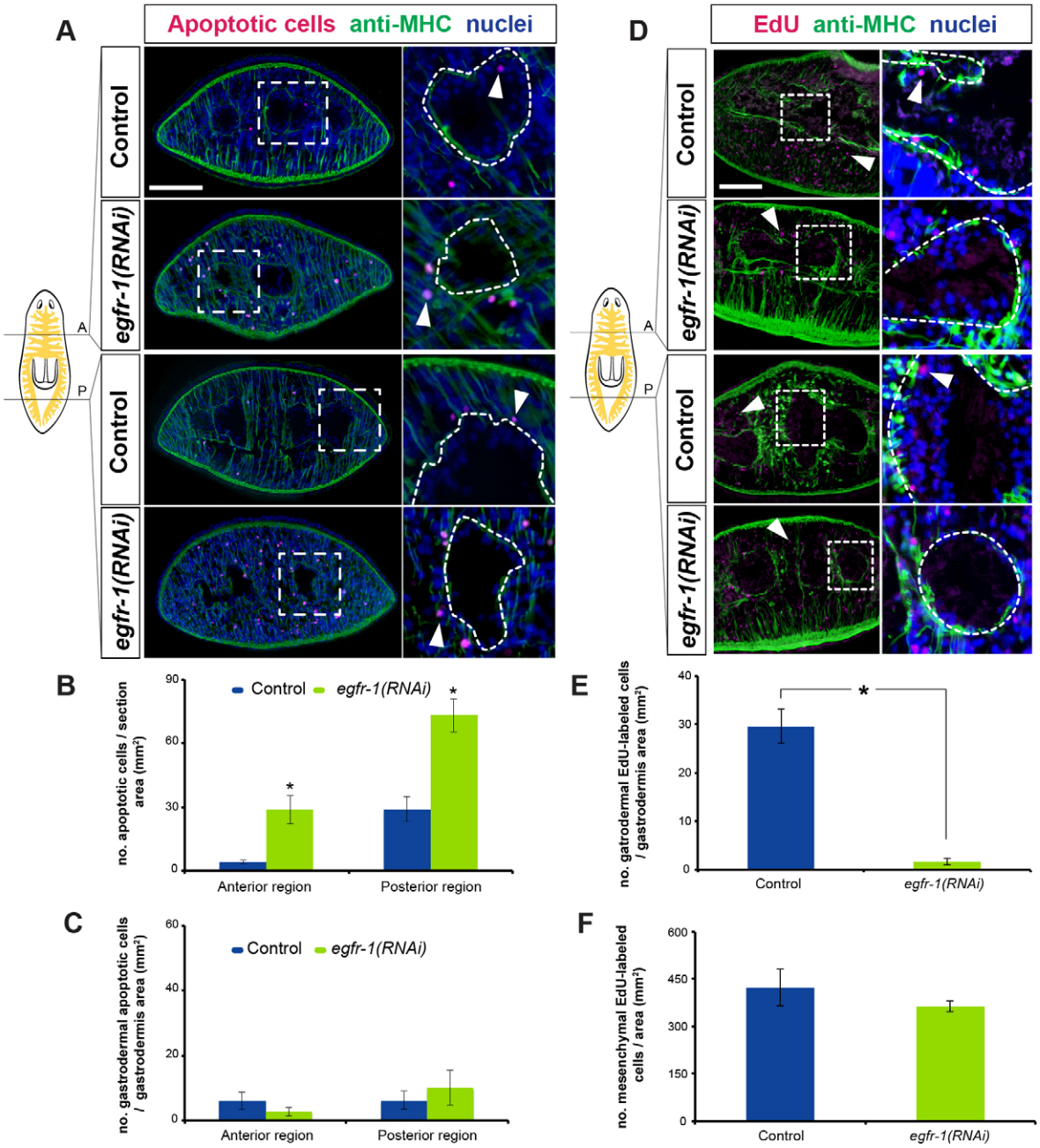

Fig. 5. Unaltered apoptosis and reduced differentiation in the gastrodermis of *egfr-1(RNAi)* animals. (A) TUNEL staining of apoptotic cells in transverse sections combined with immunohistochemistry with anti-MHC. Boxed regions are magnified on the right (dashed lines delimit the gastrodermis; white arrowheads indicate apoptotic cells). (B,C) Quantification of apoptotic cells within the mesenchyme (B) and the gastrodermis (C) in control and *egfr-1(RNAi)* animals. (D) EdU labeling in transverse sections combined with immunohistochemistry with anti-MHC. Boxed regions are magnified on the right; white arrowheads indicate EdU^+ cells (dashed lines delimit the gastrodermis). (E,F) Quantification of EdU^+ cells within the gastrodermis (E) and mesenchyme (F) in control and *egfr-1(RNAi)* animals. For all statistical analyses n=5 animals, with 5 sections analyzed per animal and position. Error bars represent the s.e.m. *P<0.05 (Student's t-test). In all panels nuclei are counterstained with DAPI and the dorsal aspect is oriented towards the top. Scale bars: 100 µm.

By contrast, there were no significant differences in the number of mesenchymal EdU-labeled cells between control and *egfr-1(RNAi)* animals (Fig. 5F). These findings suggest that the reduced number of gastrodermal cells in *egfr-1(RNAi)* animals is likely to be due to impaired differentiation of gut progenitor cells.

egfr-1 silencing increases the number of gut progenitor cells

Because neoblasts are the only source of new gastrodermal cells (Forsthoefel et al., 2011), we hypothesized that abnormal neoblast proliferation and/or commitment dynamics could account for the impaired differentiation observed in *egfr-1(RNAi)* animals. In agreement with previous studies (Fraguas et al., 2011), we found that neoblast proliferation was significantly increased in *egfr-1 (RNAi)* animals (Fig. S1A,B). Moreover, we observed a clear increase in the total number of neoblasts, as determined using the specific marker *histone-2B* (Solana et al., 2012) (Fig. S1C), the anti-SMEDWI-1 antibody (Fig. S1D) and *smedwi-1* (Fig. S1E,F).

Development (2016) 143, 2089-2102 doi:10.1242/dev.131995

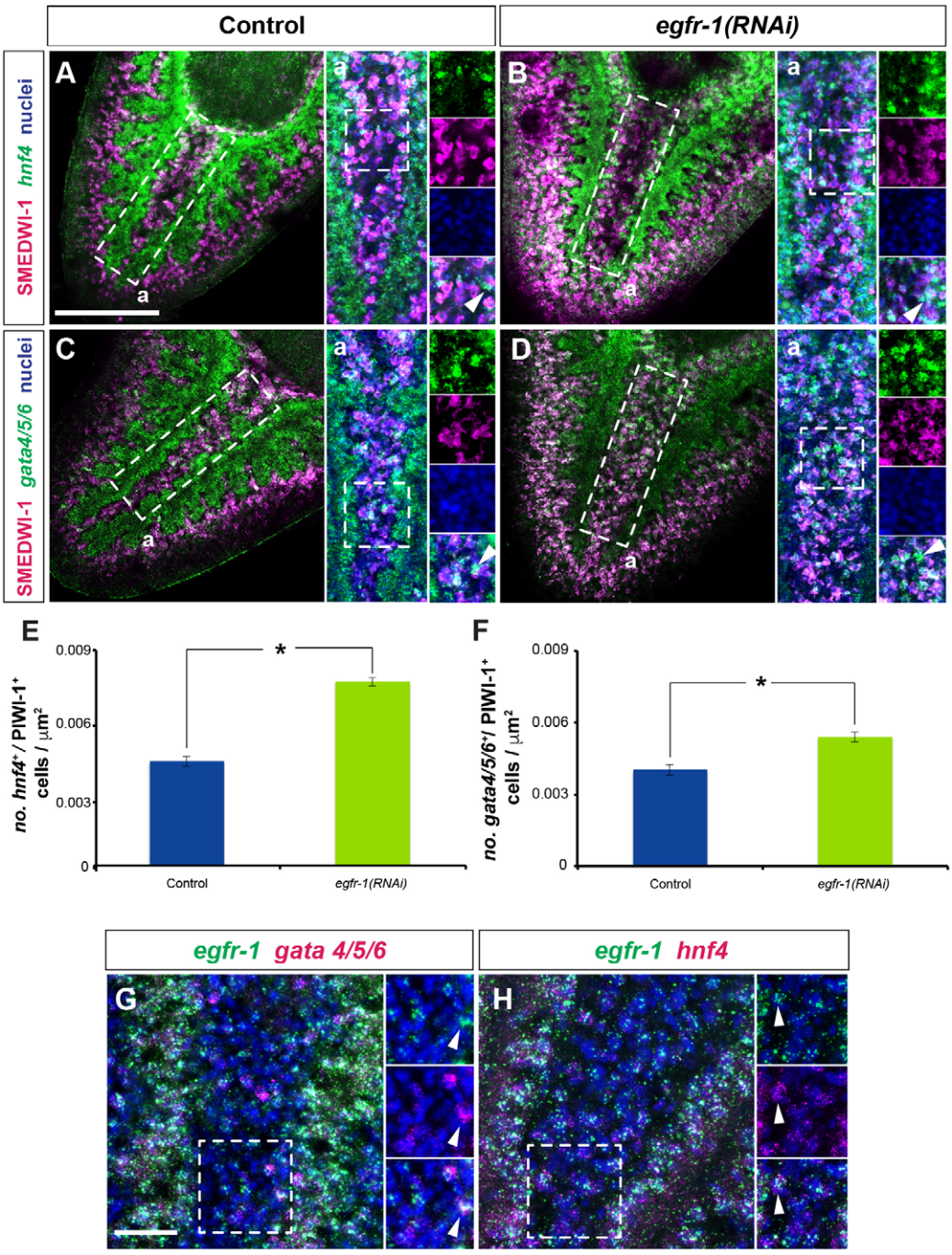

Fig. 6. Increased gut progenitor population in *egfr-1(RNAi)* animals. (A-D) Whole-mount fluorescent *in situ* hybridizations of *hnf4* (A,B) and *gata4/5/6* (C,D) combined with immunohistochemistry for SMEDWI-1. Panels Aa-Da are magnifications of boxed regions in A-D. Dashed squares in these panels are magnified on the right-hand side for better visualization of *hnf4*$^+$/SMEDWI-1$^+$ and *gata4/5/6*$^+$/SMEDWI-1$^+$ cells (arrowheads). (E,F) Significant increase in the number of *hnf4*$^+$/SMEDWI-1$^+$ (E) and *gata4/5/6*$^+$/SMEDWI-1$^+$ cells (F) after *egfr-1* RNAi. (G,H) Overlay of *egfr-1* expression with that of *gata4/5/6* (G) and *hnf4* (H). The boxed regions are magnified on the right to show the colocalization of *egfr-1* and *hnf4* or *gata456* in certain cells (arrowheads). In all statistical analyses n=10 animals. Error bars represent s.e.m. *P<0.05 (Student's t-test). In all panels, nuclei are counterstained with TO-PRO-3 and the anterior end is oriented towards the top. Scale bars: 200 µm in A (applies to A-D); 50 µm in G,H.

The expanded neoblast population observed in *egfr-1(RNAi)* animals allowed us to rule out defective stem cell maintenance as a possible source of the *egfr-1* RNAi phenotype and to consider the possibility of impaired commitment of neoblasts to intestinal progenitors. The transcription factors *hnf4* and *gata4/5/6* are expressed by differentiated gut cells and by a sub-class of neoblasts (γ-neoblasts) (van Wolfswinkel et al., 2014) proposed to be progenitors of this cell lineage (Scimone et al., 2014; Wagner et al., 2011). Therefore, we quantified the number of *hnf4*$^+$/SMEDWI-1$^+$ and *gata4/5/6*$^+$/SMEDWI-1$^+$ cells in control and *egfr-1(RNAi)* animals (Fig. 6). Silencing of *egfr-1* resulted in a significant increase in the number of both *hnf4*$^+$/SMEDWI-1$^+$ (Fig. 6A,B,E) and *gata4/5/6*$^+$/SMEDWI-1$^+$ (Fig. 6C,D,F) cells. Moreover, we observed co-expression of *egfr-1* and *gata4/5/6*

Development (2016) 143, 2089-2102 doi:10.1242/dev.131995

(Fig. 6G), as well as *egfr-1* and *hnf4* (Fig. 6H) in mesenchymal cells. Altogether, these results suggest that the gastrodermis defects observed in *egfr-1(RNAi)* animals are due to impaired differentiation of gut progenitors into mature gastrodermal cells rather than in their commitment to this cell lineage.

Silencing of the putative ligand *nrg-1* phenocopies the defects observed in *egfr-1(RNAi)* animals

To date, only one putative EGF ligand, *epiregulin-1*, has been identified in planarians. Its expression is limited to the digestive system (Wenemoser et al., 2012) (Fig. S2A) and its silencing failed to affect gut regeneration or homeostasis (Fig. S2B). We thus performed new *in silico* searches and identified a new putative EGF ligand, which we named *nrg-1* (Fig. S3). In intact animals, *nrg-1* was mainly expressed in the mesenchyme and pharynx (Fig. 7A). During regeneration, *nrg-1* was expressed within blastemas from 3 days onwards, as well as in the mesenchyme and the newly regenerating pharynx (Fig. 7A). *nrg-1* RNAi affected both regeneration (Fig. 7B,C) and homeostasis (Fig. 7D-G), phenocopying the defects observed after *egfr-1* knockdown (Fraguas et al., 2011). After *nrg-1* RNAi, regenerating head pieces formed smaller pharynxes than controls, although the pre-existing pharynx of trunk pieces appeared unaffected, as evidenced by the expression profile of the specific marker *laminin* (Cebrià and Newmark, 2007) (Fig. 7B-C). Regenerating *nrg-1(RNAi)* trunks formed smaller eye pigment cups than those seen in controls (Fig. 7B). Consistent with our observations in *egfr-1(RNAi)* animals, *nrg-1(RNAi)* animals were unable to regenerate new gut branches and gradually lost the pre-existing branches (Fig. 7C). Furthermore, an increase in the neoblast population was observed in regenerating *nrg-1(RNAi)* animals (Fig. 7C).

During homeostasis, *nrg-1* RNAi led to a reduction in the number of eye pigment cells (Fig. 7D), although the pharynx appeared unaffected (Fig. 7E). We also observed fewer gut branches in *nrg-1 (RNAi)* animals compared with controls (Fig. 7E), although these defects were milder than those seen in the pre-existing tissue of regenerating animals (Fig. 7C). Finally, as in regenerating animals, the neoblast population was increased (Fig. 7E-G). Two rounds of dsRNA injection in both regenerating (Fig. S4A) and homeostatic animals (Fig. S4B) led to more severe defects in the pharynx, eyes and gut, and ultimately to death of the animal after a few days. Our functional analyses revealed that *nrg-1(RNAi)* animals exhibit a phenotype strikingly similar to that of *egfr-1(RNAi)* animals, supporting the view that *nrg-1* might act via *egfr-1*.

If *nrg-1* does indeed activate *egfr-1*, a reduction in gut cell differentiation and an increase of the pool of gut progenitors (γ-neoblasts) would be expected after *nrg-1* silencing. To investigate this hypothesis, we labeled S-phase neoblasts in control and *nrg-1 (RNAi)* animals 20 days after a single round of dsRNA injection. After a 6-day chase, we observed a significant reduction of EdU incorporation in the gut tissue of *nrg-1(RNAi)* animals compared with controls (Fig. 8A,B). By contrast, no significant differences in the number of mesenchymal EdU-labeled cells were observed (Fig. 8C). Next, we assessed the γ-neoblast population by quantifying the number of *hnf4*$^{+}$/SMEDWI-1^{+} and *gata4/5/6*$^{+}$/SMEDWI-1^{+} cells in controls and in *nrg-1(RNAi)* animals (Fig. 8D-I). As predicted, *nrg-1* silencing resulted in a significant increase in the number of *hnf4*$^{+}$/SMEDWI-1^{+} cells (Fig. 8D,E,H). However, no significant differences in the number of *gata4/5/6*$^{+}$/SMEDWI-1^{+} cells (Fig. 8F,G,I) were observed, probably because the gut defects were less severe after only one round of *nrg-1* inhibition. Overall, these results suggest that the gut defects observed in *nrg-1(RNAi)* animals are due to impaired differentiation of neoblasts into gastrodermal cells, further supporting our hypothesis that the putative EGF ligand *nrg-1* controls differentiation of gut progenitors via *egfr-1*.

Silencing of *egfr-1* and *nrg-1* induces an increase in the expression of σ- and ζ-neoblast markers, but exclusively affects gastrodermal cell differentiation

To elucidate how the general increase in the neoblast population in *egfr-1(RNAi)* and *nrg-1(RNAi)* animals affected the primary neoblast subclasses σ and ζ, we performed whole-mount *in situ* hybridizations with the σ-neoblast marker *soxP-2* and the ζ-neoblast marker *zfp-1* (van Wolfswinkel et al., 2014). We observed an apparent increase in both neoblast subclasses in *egfr-1(RNAi)* and *nrg-1(RNAi)* animals (Fig. S5A,D). qPCR analysis of *soxP-2* and *zfp-1* expression levels revealed a significant increase in the expression of both σ- and ζ-neoblasts in *egfr-1 (RNAi)* animals (Fig. S5B,C), but only in ζ-neoblasts in *nrg-1(RNAi)* animals (Fig. S5E,F). These results demonstrate that the expansion of the neoblast population observed after silencing of *egfr-1* and *nrg-1* affects all described primary neoblast subclasses.

To determine whether this expansion of the neoblast population affected other cell lineages, we analyzed a set of known markers of differentiated cells and progenitor cells from diverse planarian tissues. We observed no significant differences in the populations of dopaminergic (*th*) (Nishimura et al., 2007) or octopaminergic (*tbh*) (Nishimura et al., 2008) neurons between control and *egfr-1(RNAi)* animals (Fig. S6A-C), and no change in the expression of the neural progenitor marker *coe* (Cowles et al., 2013) (Fig. S6A). Analysis of the expression of the protonephridial cell marker *CAVII-1* (Sánchez Alvarado et al., 2002) and the excretory system progenitor marker *pou2/3* (Scimone et al., 2011) revealed no differences between control and *egfr-1(RNAi)* animals (Fig. S6D,E). Similarly, expression of the epithelial lineage-specific marker *AGAT-1* (Eisenhoffer et al., 2008; Tu et al., 2015) did not differ significantly between control and *egfr-1(RNAi)* animals (Fig. S6F,G). Similar results were obtained after *nrg-1* silencing (Fig. S7). Altogether, these data suggest that the observed expansion of the neoblast population seen after both *egfr-1* and *nrg-1* RNAi does not affect the commitment/differentiation of neural, epidermal or excretory cell lineages.

Finally, because pharynx regeneration and maintenance is also impaired in *egfr-1* and *nrg-1* RNAi animals (Fraguas et al., 2011), we sought to determine whether those alterations were attributable to an impaired differentiation of new pharyngeal cells. Both *egfr-1 (RNAi)* and *nrg-1(RNAi)* animals showed statistically similar numbers of EdU^{+} cells within this organ (Fig. S8A-D). Analysis of the expression of the pharynx-progenitor marker *foxA* (Adler et al., 2014) showed no significant differences between treated animals and controls (Fig. S8E,F). Taken together, these results suggest that *egfr-1* and *nrg-1* are implicated in pharynx regeneration and homeostasis via a mechanism other than neoblast differentiation.

DISCUSSION

egfr-1 and *nrg-1* regulate gut regeneration and homeostasis

Gut regeneration relies on both remodeling of the pre-existing gastrodermis and the supply of newly differentiated gut cells (Forsthoefel et al., 2011). This *de novo* differentiation occurs within the blastema, as well as in other regions of the pre-existing intestine that need to remodel the normal proportions and symmetry of this organ (Forsthoefel et al., 2011). Our results uncover a new function

Development (2016) 143, 2089-2102 doi:10.1242/dev.131995

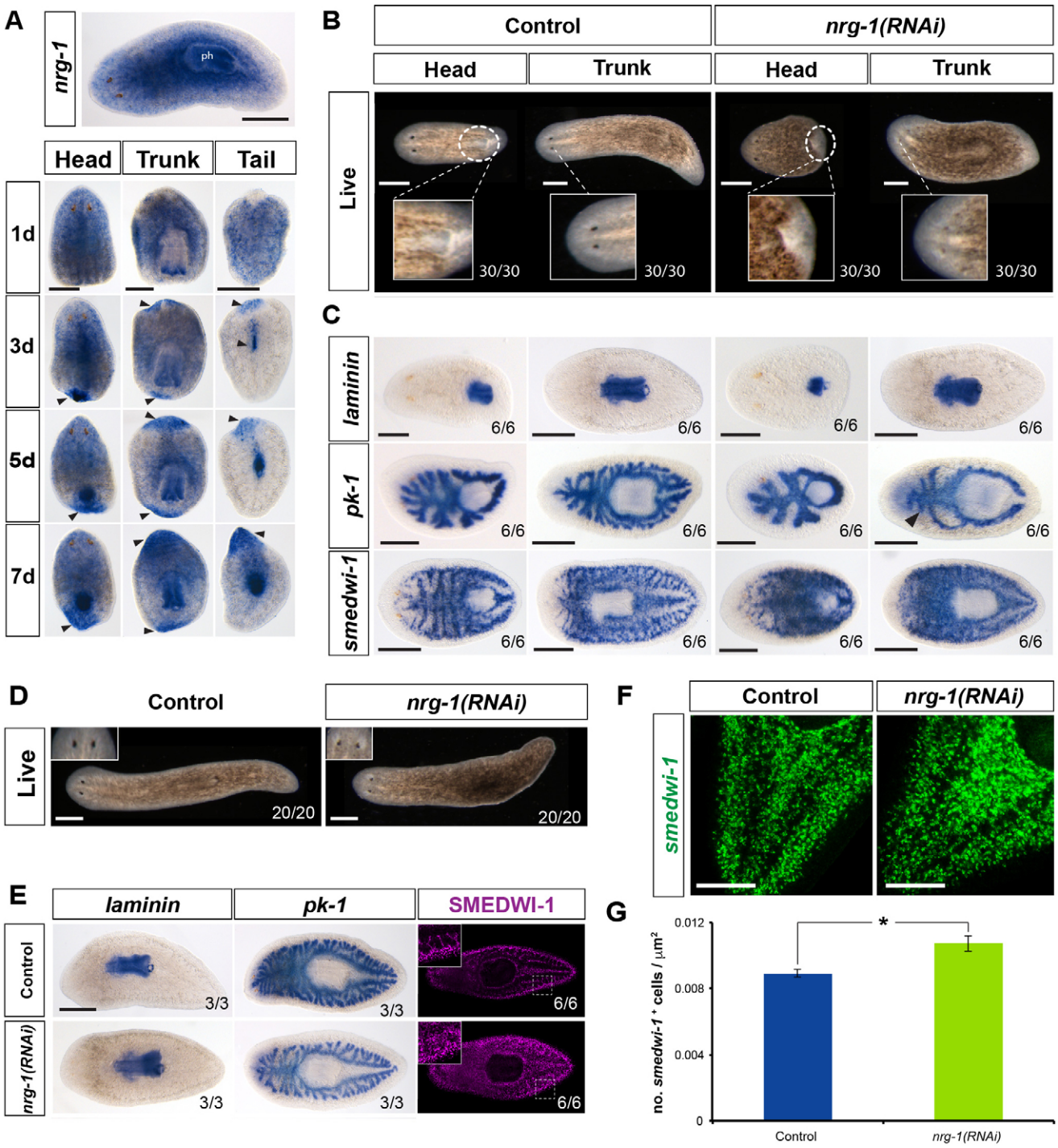

Fig. 7. *nrg-1* expression and RNAi phenotype. (A) Whole-mount *in situ* hybridizations of *nrg-1* in intact and regenerating animals (regeneration time is indicated on the left). Arrowheads indicate *nrg-1* expression in blastemas. *nrg-1(RNAi)* phenotype in regenerating (B,C) and intact (D-G) animals. *nrg-1(RNAi)* animals have reduced eye pigment cups (magnifications in B and D) and defective regeneration and homeostasis in the pharynx and gut (C-E). Increase in the population of neoblasts, stained with *smedwi-1* (C,F) and SMEDWI-1 (E). (G) Significant increase in the number of *smedwi-1*$^{+}$ cells in intact *nrg-1(RNAi)* animals. For statistical analyses, n=10 animals. Error bars represent s.e.m. *P<0.05 (Student's t-test). In all panels the anterior end is oriented to the left. Scale bars: 500 µm in B,D; 300 µm in A,C,E; 200 µm in F.

of *egfr-1* and *nrg-1* in controlling regeneration of the planarian gut and maintaining the morphology of the pre-existing tissue. In *egfr-1 (RNAi)* animals, pre-existing primary branches are partially capable of elongation during the first week after amputation, suggesting that the contribution of the differentiated tissue to gut regeneration is not impaired. Accordingly, the incomplete elongation of the primary branches and the failure to form new secondary and tertiary branches, together with the marked defects in remodeling of the pre-existing gastrodermis, are consistent with compromised differentiation of new gastrodermal cells in these animals.

During planarian homeostasis, adult tissues preserve their shape and integrity through cell turnover, which involves the constant

Development (2016) 143, 2089-2102 doi:10.1242/dev.131995

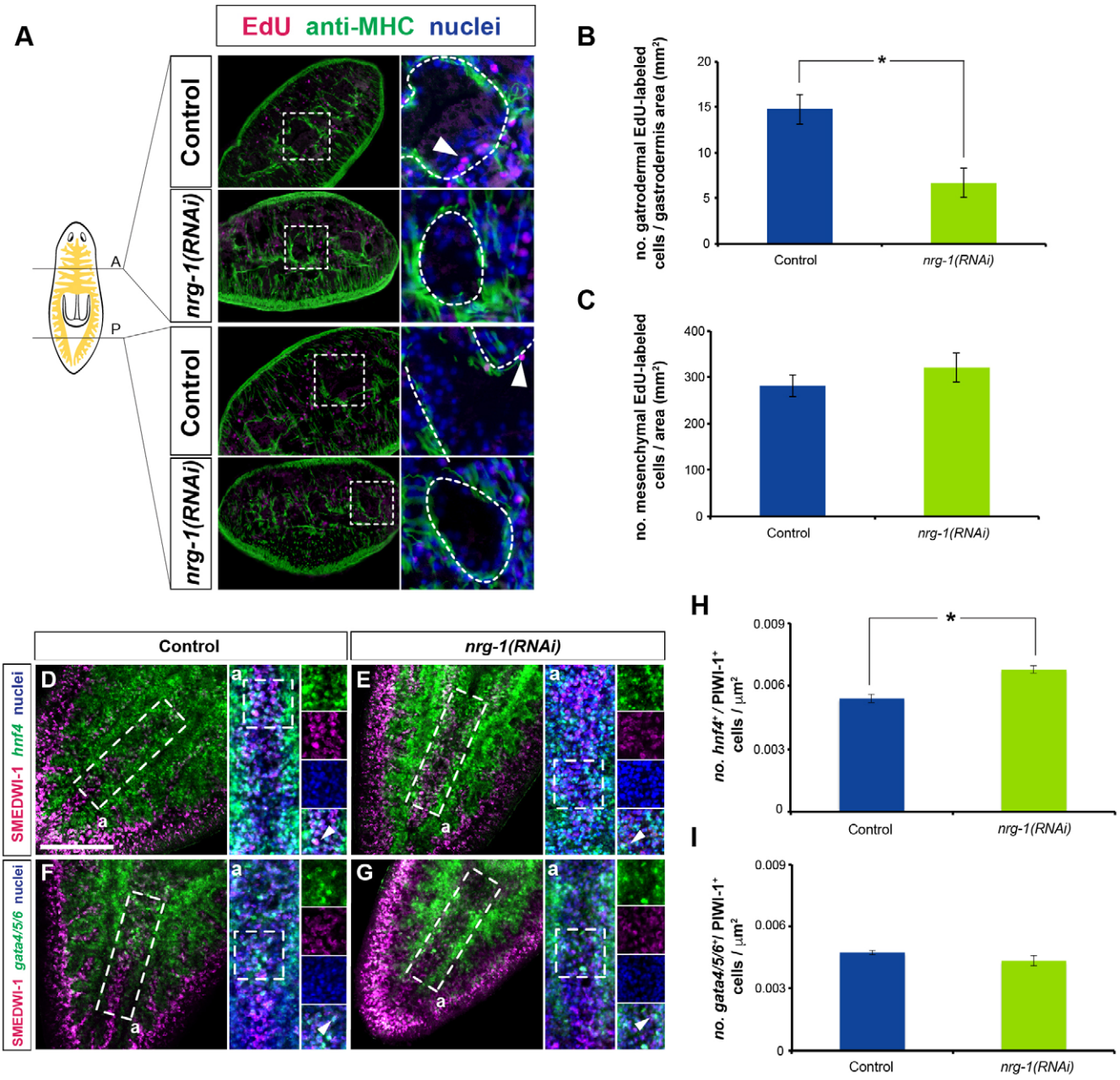

Fig. 8. Reduced gastrodermal differentiation and increased *hnf4*$^{+}$ progenitor population in *nrg-1(RNAi)* animals. (A) EdU labeling in transverse sections combined with immunohistochemistry with anti-MHC. Boxed regions are magnified on the right. White arrowheads indicate EdU^{+} cells within the gastrodermis (delimited by dashed lines). (B,C) Quantification of EdU^{+} cells within the gastrodermis (B) and mesenchyme (C) in control and *nrg-1(RNAi)* animals. (D-G) Whole-mount fluorescent *in situ* hybridizations of *hnf4* (D,E) and *gata4*/*5*/*6* (green) (F,G), combined with immunohistochemistry with SMEDWI-1 antibody. Panels Da-Ga are magnifications of boxed regions. Dashed boxes are magnified on the right for better visualization of *hnf4*$^{+}$/SMEDWI-1^{+} and *gata4*/*5*/*6*$^{+}$/SMEDWI-1^{+} cells (arrowheads). (H,I) Quantification of *hnf4*$^{+}$/SMEDWI-1^{+} (H) and *gata4*/*5*/*6*$^{+}$/SMEDWI-1^{+} cells (I) after *nrg-1* RNAi. For EdU statistical analyses, *n*=5 animals, with 5 sections analyzed per animal and position. For *hnf4*$^{+}$and *gata4*/*5*/*6*$^{+}$statistical analyses, *n*=7 animals. In all cases, error bars represent the s.e.m. **P*<0.05 (Student's *t*-test). Nuclei are counterstained with DAPI in A and with TO-PRO-3 in D-G. Dorsal aspect is oriented towards the top in A and the anterior end towards the top in D-G. Scale bars: 100 µm in A; 200 µm in D (applies to D-G).

death of differentiated cells, the division of ASCs, and the differentiation and integration of ASC progeny into the pre-existing tissue to replace the lost cells (Pellettieri and Sánchez Alvarado, 2007). In the planarian gut, the uniform integration of new gastrodermal cells throughout the intestine maintains this tissue and contributes to the formation of new gut branches, which are always in proportion to the animal's body size (Forsthoefel et al., 2011). Silencing of *egfr-1* and *nrg-1* impairs the differentiation of new gut cells. This, together with a normal ratio of cell loss by apoptosis, disrupts the normal turnover of the gut in *egfr-1(RNAi)* animals, compromising maintenance of its normal morphology. Accordingly, the defects in gut tissue are observed gradually, from the most terminal branches (i.e. quaternary and tertiary), which consist of fewer cells, to the most principal branches, which contain a larger number of gastrodermal cells. Notably, this phenotype differs from those described after silencing other genes required for

Development (2016) 143, 2089-2102 doi:10.1242/dev.131995

intestinal integrity (Forsthoefel et al., 2012). The impairment of intestinal adhesion, polarity and phagocyte maturation completely compromises gut regeneration and homeostasis, eventually leading to the death of the animal (Forsthoefel et al., 2012).

The EGFR pathway controls the differentiation of gut progenitor cells

Planarian neoblasts are heterogeneous, consisting of pluripotent ASCs and lineage-committed progenitors (Scimone et al., 2014; van Wolfswinkel et al., 2014). Gene expression profiling shows the existence of three subclasses of neoblasts: ζ-neoblasts, regarded as a epidermal progenitors (Tu et al., 2015; van Wolfswinkel et al., 2014); γ-neoblasts, identified by the expression of the endodermal transcription factors *hnf4* and *gata4/5/6* (Ang et al., 1993; Azzaria et al., 1996; Murakami et al., 2005), and thus hypothesized to include gut progenitors (van Wolfswinkel et al., 2014); and σ-neoblasts, which are regarded as truly pluripotent neoblasts with the ability to generate all the other subclasses and cell lineages (van Wolfswinkel et al., 2014). In addition to these advances, recent studies have begun to elucidate the process by which neoblast dynamics are regulated. The RNA-binding protein *mex3-1* (Zhu et al., 2015) and the transcription factor *egr-5* (Tu et al., 2015) are key regulators of the specification of all major known lineage progenitors and the differentiation of the epidermal lineage, respectively.

Our results indicate that *egfr-1* and *nrg-1* are essential regulators of the differentiation of gut progenitors into mature gastrodermal cells. Remarkably, the specification of gut progenitors (γ-neoblasts) is not affected after silencing of *egfr-1* and *nrg-1*, and the expansion of this population is probably due to their incapacity to differentiate. This phenomenon is reminiscent of the phenotype observed after *egr-5* silencing, whereby epidermal differentiation is impaired whereas numbers of epidermal progenitors increase (Tu et al., 2015). Importantly, the analysis of other differentiated cell/progenitor populations, including epidermal, excretory, neural and pharyngeal cells, suggests that the silencing of *egfr-1* and *nrg-1* specifically affects differentiation of the gut lineage. We thus propose that in normal conditions, pluripotent neoblasts commit to gut progenitors and start expressing *hnf4* and/or *gata4/5/6* with *egfr-1*. Upon *nrg-1* binding, these cells proceed to differentiate into mature gut cells (Fig. 9A). Silencing of either *egfr-1* or its putative

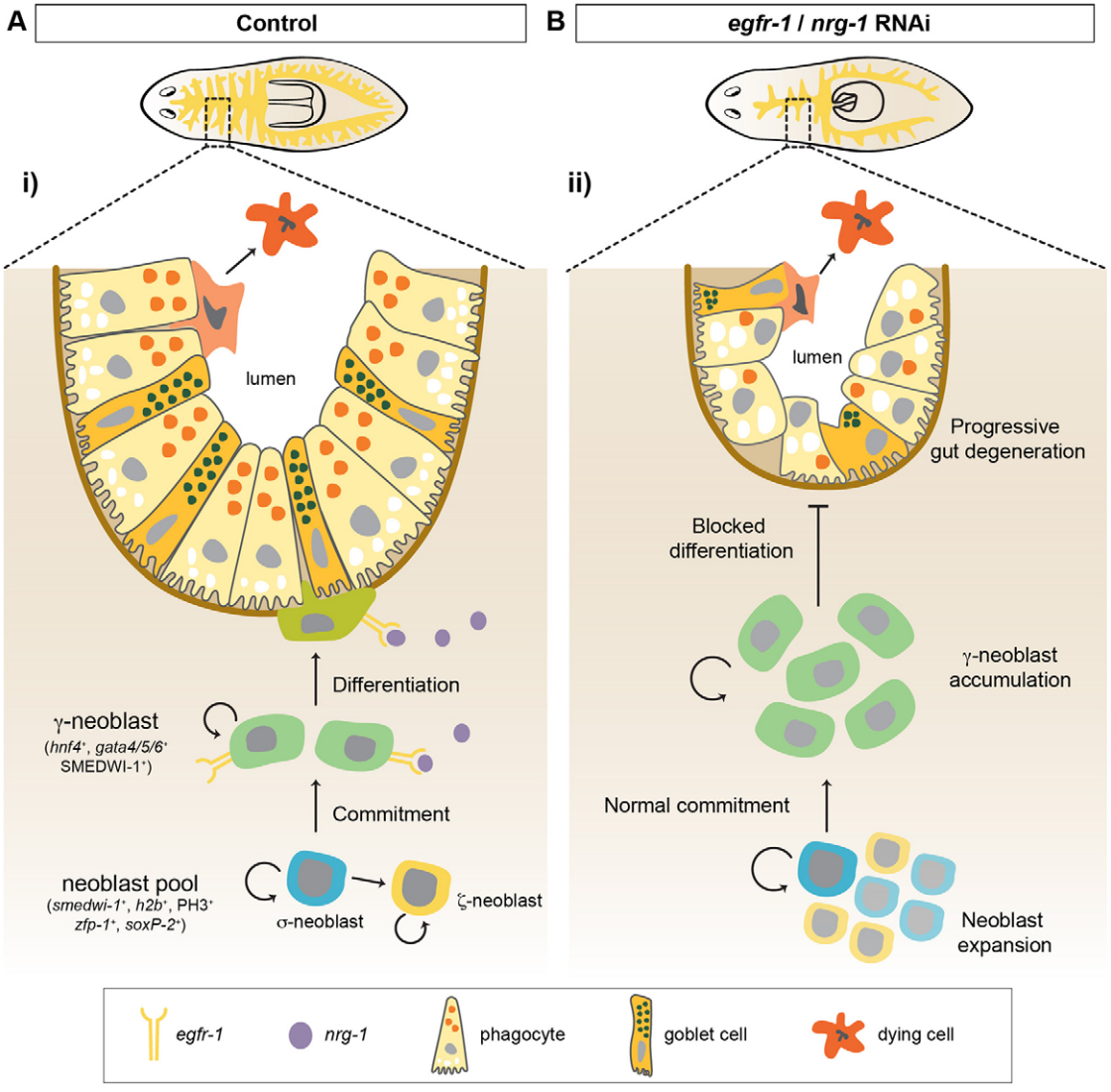

Fig. 9. Model for the role of *egfr-1* and *nrg-1* in the planarian gut. (A) Normal gut cell turnover. (B) Impaired gut cell turnover after the silencing of either *egfr-1* or *nrg-1*. See details in the text.

Development (2016) 143, 2089-2102 doi:10.1242/dev.131995

ligand *nrg-1* disrupts EGFR signaling, and hence the differentiation of gut progenitors, leading to their accumulation in the mesenchyme (Fig. 9B). However, several aspects of this scenario require further study, such as the cellular origin of *nrg-1*, the dynamics of *nrg-1/egfr-1* binding, and the mechanisms underlying *nrg-1* proteolysis and diffusion. Finally, the EGF receptors *egfr-3* and *egfr-5* control the regeneration and homeostasis of particular planarian cell types, such as neuronal and excretory cells (Fraguas et al., 2011; Rink et al., 2011). Further studies will thus help us to elucidate whether the model proposed here can be extrapolated to these other receptors, eventually uncovering a general role of the planarian EGFR pathway in the regulation of progenitor cell differentiation.

Strikingly, the silencing of *egfr-1* and *nrg-1* also results in the hyperproliferation and expansion of the ζ- and σ-neoblasts. However, this neoblast expansion does not appear to correlate with an increase in the number of differentiated cells of any of the cell lineages examined. One possibility is that the loss of gut tissue stimulates neoblasts to proliferate as part of a stress response (Tu et al., 2015). Alternatively, gut loss and disorganization could affect some signaling processes, normally originating in the gastrodermis, that regulate neoblast dynamics (Adler and Sánchez Alvarado, 2015). The latter possibility is supported by a study of transcription factor *nkx-2.2*. Silencing of this gene, which is expressed in the gut, disrupts gut integrity and blocks neoblast proliferation (Forsthoefel et al., 2012). Accordingly, future studies will need to elucidate the precise causes of this hyperproliferation and determine whether the observed increased in apoptosis in the mesenchyme reflects a compensatory response to this increase.

In summary, our study uncovers a role of the EGFR signaling pathway in controlling the differentiation of gut progenitors in the planarian *S. mediterranea*. This role in stem cell differentiation appears to be widespread among bilaterian animals (Freeman et al., 1992; Galvez-Contreras et al., 2015; Yoo et al., 2004). Moreover, studies performed in *Drosophila* and mouse have demonstrated the role of the EGFR pathway in the maintenance of the intestine (Jiang et al., 2011; Wong et al., 2012), as demonstrated here in planarians. However, contrary to our observations, the EGFR pathway appears to regulate the proliferation of intestinal stem cells in the aforementioned organisms. Therefore, our results support a conserved role of this pathway in controlling the dynamics of ASCs in bilaterian animals and underscore the utility of the unique planarian ASC system as a model in which to study the role of the EGFR pathway in stem cell biology.

MATERIALS AND METHODS

Planarian culture

Asexual *S. mediterranea* from the BCN-10 clonal line were maintained in artificial water (Cebrià and Newmark, 2005). Animals were fed with veal liver and starved for at least 1 week before all experiments.

Gene identification and cloning

All genes were amplified by gene-specific PCR and cloned into either pCRII (Life Technologies) or pGEM-T Easy (Promega) vectors. The putative EGF ligand *nrg-1* was identified by *in silico* searches querying *Prostheceraeus vittatus* putative EGF ligands (BioProject accession ID: PRJNA277637).

RNA interference

Silencing by RNAi was performed as previously described (Sánchez Alvarado and Newmark, 1999) and validated by qPCR (Fig. S9). Control animals were injected with double-stranded RNA (dsRNA) for green fluorescent protein (GFP). In *egfr-1(RNAi)* analyses, all animals received two rounds of injections separated by 3-4 days, whereas only one round of injections was performed for *nrg-1(RNAi)* analyses.

Quantitative real-time PCR

Total RNA was extracted from a pool of five control, *egfr-1(RNAi),* and *nrg-1(RNAi)* animals. Quantitative real-time PCR was performed as described previously (Solana et al., 2012) and data were normalized based on the expression of the internal control URA-4. All experiments were performed using three biological and three technical replicates for each condition. The following primers (5′ to 3′) were used: *egfr-1F*, CTGATTGGAAAGGATGTACTCAATGT; *egfr-1R*, ACCATTACACTGCGGATGACAC; *nrg-1F*, TGACGAATCTAGAAGGAAATGTAGC; *nrg-1R*, CGACGTCCGTAGAAACCATTT; *soxP-2F,* CCAGCAATTTTCCCAAAG; *soxP-2R*, CCCCTTCTGAATCATCCAT; *zfp-1F*, AAATTTTCCCGTGCCTG; *zfp-1R*, TGATCTTTGAGTGAAGCTGGT.

Whole-mount *in situ* hybridization and immunohistochemistry

Single and double fluorescent *in situ* hybridizations (FISH) were performed as previously described (King and Newmark, 2013) using the Tyramide Signal Amplification Kit (TSA; Perkin Elmer). After probe development, neoblasts were visualized with rabbit anti-SMEDWI-1 antibody (kindly provided by Kerstin Bartscherer, Max Planck Institute for Molecular Biomedicine, Münster, Germany; 1:1100) (Guo et al., 2006; Marz et al., 2013).

In situ hybridization, immunohistochemistry and histological staining of paraffin sections

For *in situ* hybridization and immunohistochemistry, animals were killed in 2% HCl in Milli-Q water, fixed with 4% paraformaldehyde in PBS for 4 h at 4°C, and stored in 70% ethanol in Milli-Q water. Paraffin embedding, sectioning, and subsequent *in situ* hybridization and immunostaining were performed as previously described (Adell et al., in press; Cardona et al., 2005a). The antibodies used were rabbit anti-SMEDWI-1 (1:1100), mouse anti-MHC (kindly provided by Rafael Romero, University of Barcelona, Spain; 1:20) (Cebrià et al., 1997), anti-phospho-histone-H3-Ser10 (anti-PH3) (Cell Signaling, #3377S; 1:300) and rabbit anti-RPZ-1 (kindly provided by Kerstin Bartscherer; 1:200) (Reuter et al., 2015). Mallory's staining was performed as previously described (Cardona et al., 2005b; Sluys, 1989).

TUNEL and EdU staining of paraffin sections

Animals were fixed and sectioned as described above. Staining of apoptotic cells was performed in accordance with the manufacturer's recommendations (ApopTag Red In Situ Apoptosis Detection Kit, Merck-Millipore, S7165), followed by immunostaining with anti-MHC (as described above). Samples were counterstained with DAPI (1:5000 in PBS) and mounted with 70% glycerol in PBS. For EdU experiments, a single pulse of F-ara-Edu (Sigma) was injected into control, *egfr-1(RNAi)* and *nrg-1(RNAi)* animals at a concentration of 60 µg/ml (diluted in 10% DMSO/planarian artificial water). After a 6-day chase, staining of EdU-labeled cells was performed using the EdU Click-555 kit (Baseclick, BCK-EdU555), following the manufacturer's recommendations, with the addition of a prior step consisting of incubation in proteinase K (20 µg/ml) for 10 min. Samples were counterstained with anti-MHC and DAPI, and mounted in 70% glycerol in PBS.

Imaging

FISH samples were imaged under either a MZ16F stereomicroscope (Leica) equipped with a ProgRes C3 camera (Jenoptik) or an SPE confocal laser-scanning microscope (Leica). Histological sections were observed under an Axiophot microscope (Zeiss) and imaged with a DFC300FX camera (Leica) or an SP2 confocal laser-scanning microscope (Leica). Images were processed using Fiji and Photoshop CS6 (Adobe) software. Brightness/contrast and color balance adjustments were always applied to the entire image, rather than specific regions thereof.

Acknowledgements

We thank José M. Martín-Durán and all the members of Emili Saló's lab for support and discussion. We thank Kerstin Bartscherer for the anti-SMEDWI-1 and the anti-RPZ-1 antibodies, and Rafael Romero for the anti-MHC antibody. We thank Owen Howard for advice on English style.

Competing interests
The authors declare no competing or financial interests.

Author contributions
S.B. and F.C. conceived and designed the study. S.B. and S.F. conducted the experiments and S.B. drafted the manuscript. All authors discussed and commented on the data. F.C. edited the paper.

Funding
This study was funded by the Ministerio de Economía y Competitividad (MICINN, Spain) [BFU2011-22510 and BFU2012-31701]; and Generalitat de Catalunya [2009-SGR-1018 to F.C.]. S.B. was supported by a fellowship from the Generalitat de Catalunya and a collaboration fellowship from the Institute of Biomedicine of the University of Barcelona (IBUB). S.F. was supported by a fellowship from MICINN.

Data availability
The sequence of *smed-nrg-1* has been deposited in GenBank with accession number KU850495.

Supplementary information
Supplementary information available online at
http://dev.biologists.org/lookup/suppl/doi:10.1242/dev.131995/-/DC1

References
Adell, T., Barberán, S., Sureda-Gómez, M., Almuedo-Castillo, M., De Sousa, N. and Cebrià, F. (2016). Immunohistochemical protocols for paraffin-embedded tissue sections in planarians. *Methods Mol. Biol*. (in press).
Adler, C. E. and Sánchez Alvarado, A. (2015). Types or States? Cellular dynamics and regenerative potential. *Trends Cell Biol.* **25**, 687-696.
Adler, C. E., Seidel, C. W., McKinney, S. A. and Sánchez Alvarado, A. (2014). Selective amputation of the pharynx identifies a FoxA-dependent regeneration program in planaria. *eLife* **3**, e02238.
Aguirre, A., Rubio, M. E. and Gallo, V. (2010). Notch and EGFR pathway interaction regulates neural stem cell number and self-renewal. *Nature* **467**, 323-327.
Ang, S. L., Wierda, A., Wong, D., Stevens, K. A., Cascio, S., Rossant, J. and Zaret, K. S. (1993). The formation and maintenance of the definitive endoderm lineage in the mouse: involvement of HNF3/forkhead proteins. *Development* **119**, 1301-1315.
Aroian, R. V., Koga, M., Mendel, J. E., Ohshima, Y. and Sternberg, P. W. (1990). The let-23 gene necessary for *Caenorhabditis elegans* vulval induction encodes a tyrosine kinase of the EGF receptor subfamily. *Nature* **348**, 693-699.
Azzaria, M., Goszczynski, B., Chung, M. A., Kalb, J. M. and McGhee, J. D. (1996). A fork head/HNF-3 homolog expressed in the pharynx and intestine of the *Caenorhabditis elegans* embryo. *Dev. Biol.* **178**, 289-303.
Baguña, J. (2012). The planarian neoblast: the rambling history of its origin and some current black boxes. *Int. J. Dev. Biol.* **56**, 19-37.
Baguñà, J., Saló, E. and Auladell, C. (1989). Regeneration and pattern formation in planarians. III. Evidence that neoblasts are totipotent stem cells and the source of blastema cells. *Development* **107**, 77-86.
Biteau, B. and Jasper, H. (2011). EGF signaling regulates the proliferation of intestinal stem cells in Drosophila. *Development* **138**, 1045-1055.
Bowen, I. D., Ryder, T. A. and Thompson, J. A. (1974). The fine structure of the planarian Polycelis tenuis Iijima. II. The intestine and gastrodermal phagocytosis. *Protoplasma* **79**, 1-17.
Bueno, D., Baguñà, J. and Romero, R. (1997). Cell-, tissue-, and position-specific monoclonal antibodies against the planarian *Dugesia (Girardia) tigrina*. *Histochem. Cell Biol.* **107**, 139-149.
Cardona, A., Fernández, J., Solana, J. and Romero, R. (2005a). An in situ hybridization protocol for planarian embryos: monitoring myosin heavy chain gene expression. *Dev. Genes Evol.* **215**, 482-488.
Cardona, A., Hartenstein, V. and Romero, R. (2005b). The embryonic development of the triclad Schmidtea polychroa. *Dev. Genes Evol.* **215**, 109-131.
Cebrià, F. and Newmark, P. A. (2005). Planarian homologs of netrin and netrin receptor are required for proper regeneration of the central nervous system and the maintenance of nervous system architecture. *Development* **132**, 3691-3703.
Cebrià, F. and Newmark, P. A. (2007). Morphogenesis defects are associated with abnormal nervous system regeneration following roboA RNAi in planarians. *Development* **134**, 833-837.
Cebrià, F., Vispo, M., Newmark, P., Bueno, D. and Romero, R. (1997). Myocyte differentiation and body wall muscle regeneration in the planarian *Girardia tigrina*. *Development Genes Evol.* **207**, 306-316.
Cela, C. and Llimargas, M. (2006). Egfr is essential for maintaining epithelial integrity during tracheal remodelling in Drosophila. *Development* **133**, 3115-3125.
Cowles, M. W., Brown, D. D. R., Nisperos, S. V., Stanley, B. N., Pearson, B. J. and Zayas, R. M. (2013). Genome-wide analysis of the bHLH gene family in planarians identifies factors required for adult neurogenesis and neuronal regeneration. *Development* **140**, 4691-4702.
Eisenhoffer, G. T., Kang, H. and Sánchez Alvarado, A. (2008). Molecular analysis of stem cells and their descendants during cell turnover and regeneration in the planarian *Schmidtea mediterranea*. *Cell Stem Cell* **3**, 327-339.
Forsthoefel, D. J., Park, A. E. and Newmark, P. A. (2011). Stem cell-based growth, regeneration, and remodeling of the planarian intestine. *Dev. Biol.* **356**, 445-459.
Forsthoefel, D. J., James, N. P., Escobar, D. J., Stary, J. M., Vieira, A. P., Waters, F. A. and Newmark, P. A. (2012). An RNAi screen reveals intestinal regulators of branching morphogenesis, differentiation, and stem cell proliferation in planarians. *Dev. Cell* **23**, 691-704.
Fraguas, S., Barberán, S. and Cebrià, F. (2011). EGFR signaling regulates cell proliferation, differentiation and morphogenesis during planarian regeneration and homeostasis. *Dev. Biol.* **354**, 87-101.
Fraguas, S., Barberán, S., Iglesias, M., Rodriguez-Esteban, G. and Cebrià, F. (2014). egr-4, a target of EGFR signaling, is required for the formation of the brain primordia and head regeneration in planarians. *Development* **141**, 1835-1847.
Freeman, M., Klämbt, C., Goodman, C. S. and Rubin, G. M. (1992). The argos gene encodes a diffusible factor that regulates cell fate decisions in the Drosophila eye. *Cell* **69**, 963-975.
Galvez-Contreras, A. Y., Gonzalez-Castaneda, R. E., Campos-Ordonez, T., Luquin, S. and Gonzalez-Perez, O. T. (2015). Phenytoin enhances the phosphorylation of EGFR and FGFR in the subventricular zone and promotes the proliferation of neural precursor cells and oligodendrocyte differentiation. *Eur. J. Neurosci.* **43**, 139-147.
Gentile, L., Cebria, F. and Bartscherer, K. (2011). The planarian flatworm: an in vivo model for stem cell biology and nervous system regeneration. *Dis. Model. Mech.* **4**, 12-19.
Guo, T., Peters, A. H. M. and Newmark, P. A. (2006). A Bruno-like gene is required for stem cell maintenance in planarians. *Dev. Cell* **11**, 159-169.
Hayashi, T., Shibata, N., Okumura, R., Kudome, T., Nishimura, O., Tarui, H. and Agata, K. (2010). Single-cell gene profiling of planarian stem cells using fluorescent activated cell sorting and its "index sorting" function for stem cell research. *Dev. Growth Differ.* **52**, 131-144.
Jiang, H.-S. and Wu, Y.-C. (2014). LIN-3/EGF promotes the programmed cell death of specific cells in *Caenorhabditis elegans* by transcriptional activation of the pro-apoptotic gene egl-1. *PLoS Genet.* **10**, e1004513.
Jiang, H., Grenley, M. O., Bravo, M.-J., Blumhagen, R. Z. and Edgar, B. A. (2011). EGFR/Ras/MAPK signaling mediates adult midgut epithelial homeostasis and regeneration in Drosophila. *Cell Stem Cell* **8**, 84-95.
King, R. S. and Newmark, P. A. (2013). In situ hybridization protocol for enhanced detection of gene expression in the planarian *Schmidtea mediterranea*. *BMC Dev. Biol.* **13**, 8.
Kobayashi, C., Kobayashi, S., Orii, H., Watanabe, K. and Agata, K. (1998). Identification of two distinct muscles in the planarian *Dugesia japonica* by their expression of myosin heavy chain genes. *Zoolog. Sci.* **15**, 861-869.
Lapan, S. W. and Reddien, P. W. (2012). Transcriptome analysis of the planarian eye identifies ovo as a specific regulator of eye regeneration. *Cell Rep.* **2**, 294-307.
Li, Z., Liu, S. and Cai, Y. (2015). EGFR/MAPK signaling regulates the proliferation of Drosophila renal and nephric stem cells. *J. Genet. Genomics* **42**, 9-20.
Lyons, D. A., Pogoda, H.-M., Voas, M. G., Woods, I. G., Diamond, B., Nix, R., Arana, N., Jacobs, J. and Talbot, W. S. (2005). erbb3 and erbb2 are essential for Schwann cell migration and myelination in zebrafish. *Curr. Biol.* **15**, 513-524.
Marz, M., Seebeck, F. and Bartscherer, K. (2013). A Pitx transcription factor controls the establishment and maintenance of the serotonergic lineage in planarians. *Development* **140**, 4499-4509.
Morgan, T. H. (1898). Experimental studies of the regeneration of *Planaria maculata*. *Arch. Entwickl. Mech. Org.* **7**, 364-397.
Morita, M. and Best, J. (1984). Electron microscopic studies of planarian regeneration. IV. Cell division of neoblasts in *Dugesia dorotocephala*. *J. Exp. Zool.* **229**, 425-436.
Moritz, S., Stöckle, F., Ortmeier, C., Schmitz, H., Rodríguez-Esteban, G., Key, G. and Gentile, L. (2012). Heterogeneity of planarian stem cells in the S/G2/M phase. *Int. J. Dev. Biol.* **56**, 117-125.
Morrison, S. J. and Spradling, A. C. (2008). Stem cells and niches: mechanisms that promote stem cell maintenance throughout life. *Cell* **132**, 598-611.
Murakami, R., Okumura, T. and Uchiyama, H. (2005). GATA factors as key regulatory molecules in the development of Drosophila endoderm. *Dev. Growth Differ.* **47**, 581-589.
Newmark, P. A. and Sánchez Alvarado, A. (2000). Bromodeoxyuridine specifically labels the regenerative stem cells of planarians. *Dev. Biol.* **220**, 142-153.
Newmark, P. A. and Sánchez Alvarado, A. (2002). Not your father's planarian: a classic model enters the era of functional genomics. *Nat. Rev. Genet.* **3**, 210-219.
Nishimura, K., Kitamura, Y., Inoue, T., Umesono, Y., Sano, S., Yoshimoto, K., Inden, M., Takata, K., Taniguchi, T., Shimohama, S. et al. (2007). Reconstruction of dopaminergic neural network and locomotion function in planarian regenerates. *Dev. Neurobiol.* **67**, 1059-1078.
Nishimura, K., Kitamura, Y., Inoue, T., Umesono, Y., Yoshimoto, K., Taniguchi, T. and Agata, K. (2008). Characterization of tyramine beta-hydroxylase in

Development (2016) 143, 2089-2102 doi:10.1242/dev.131995

planarian *Dugesia japonica*: cloning and expression. *Neurochem. Int.* **53**, 184-192.

Oh, J., Lee, Y. D. and Wagers, A. J. (2014). Stem cell aging: mechanisms, regulators and therapeutic opportunities. *Nat. Med.* **20**, 870-880.

Oviedo, N. J., Newmark, P. A. and Sánchez Alvarado, A. (2003). Allometric scaling and proportion regulation in the freshwater planarian *Schmidtea mediterranea*. *Dev. Dyn.* **226**, 326-333.

Pellettieri, J. and Sánchez Alvarado, A. (2007). Cell turnover and adult tissue homeostasis: from humans to planarians. *Annu. Rev. Genet.* **41**, 83-105.

Pellettieri, J., Fitzgerald, P., Watanabe, S., Mancuso, J., Green, D. R. and Sánchez Alvarado, A. (2010). Cell death and tissue remodeling in planarian regeneration. *Dev. Biol.* **338**, 76-85.

Reddien, P. W. (2013). Specialized progenitors and regeneration. *Development* **140**, 951-957.

Reddien, P. W. and Sánchez Alvarado, A. (2004). Fundamentals of planarian regeneration. *Annu. Rev. Cell Dev. Biol.* **20**, 725-757.

Reuter, H., März, M., Vogg, M. C., Eccles, D., Grifol-Boldú, L., Wehner, D., Owlarn, S., Adell, T., Weidinger, G. and Bartscherer, K. (2015). Beta-catenin-dependent control of positional information along the AP body axis in planarians involves a teashirt family member. *Cell Rep.* **10**, 253-265.

Rink, J. C. (2013). Stem cell systems and regeneration in planaria. *Dev. Genes Evol.* **223**, 67-84.

Rink, J. C., Vu, H. T.-K. and Sánchez Alvarado, A. (2011). The maintenance and regeneration of the planarian excretory system are regulated by EGFR signaling. *Development* **138**, 3769-3780.

Romero, R. and Baguñà, J. (1991). Quantitative cellular analysis of growth and reproduction in freshwater planarians (Turbellaria; Tricladida). I. A cellular description of the intact organism. *Invert. Reprod. Dev.* **19**, 157-165.

Sánchez Alvarado, A. and Newmark, P. A. (1999). Double-stranded RNA specifically disrupts gene expression during planarian regeneration. *Proc. Natl. Acad. Sci. USA* **96**, 5049-5054.

Sánchez Alvarado, A., Newmark, P. A., Robb, S. M. and Juste, R. (2002). The *Schmidtea mediterranea* database as a molecular resource for studying platyhelminthes, stem cells and regeneration. *Development* **129**, 5659-5665.

Scimone, M. L., Srivastava, M., Bell, G. W. and Reddien, P. W. (2011). A regulatory program for excretory system regeneration in planarians. *Development* **138**, 4387-4398.

Scimone, M. L., Kravarik, K. M., Lapan, S. W. and Reddien, P. W. (2014). Neoblast specialization in regeneration of the planarian *Schmidtea mediterranea*. *Stem Cell Rep.* **3**, 339-352.

Sluys, R. (1989). *A Monograph of the Marine Triclads*. Rotterdam; Brookfield: A.A. Balkema.

Solana, J., Kao, D., Mihaylova, Y., Jaber-Hijazi, F., Malla, S., Wilson, R. and Aboobaker, A. (2012). Defining the molecular profile of planarian pluripotent stem cells using a combinatorial RNA-seq, RNA interference and irradiation approach. *Genome Biol.* **13**, R19.

Tu, K. C., Cheng, L.-C., Vu, H. T. K., Lange, J. J., McKinney, S. A., Seidel, C. W. and Sánchez Alvarado, A. (2015). Egr-5 is a post-mitotic regulator of planarian epidermal differentiation. *eLife* **4**, e10501.

van Wolfswinkel, J. C., Wagner, D. E. and Reddien, P. W. (2014). Single-cell analysis reveals functionally distinct classes within the planarian stem cell compartment. *Cell Stem Cell* **15**, 326-339.

Visvader, J. E. (2011). Cells of origin in cancer. *Nature* **469**, 314-322.

Wagner, D. E., Wang, I. E. and Reddien, P. W. (2011). Clonogenic neoblasts are pluripotent adult stem cells that underlie planarian regeneration. *Science* **332**, 811-816.

Wenemoser, D., Lapan, S. W., Wilkinson, A. W., Bell, G. W. and Reddien, P. W. (2012). A molecular wound response program associated with regeneration initiation in planarians. *Genes Dev.* **26**, 988-1002.

Wong, V. W. Y., Stange, D. E., Page, M. E., Buczacki, S., Wabik, A., Itami, S., van de Wetering, M., Poulsom, R., Wright, N. A., Trotter, M. W. B. et al. (2012). Lrig1 controls intestinal stem-cell homeostasis by negative regulation of ErbB signalling. *Nat. Cell Biol.* **14**, 401-408.

Yoo, A. S., Bais, C. and Greenwald, I. (2004). Crosstalk between the EGFR and LIN-12/Notch pathways in *C. elegans* vulval development. *Science* **303**, 663-666.

Zhu, S. J., Hallows, S. E., Currie, K. W., Xu, C. and Pearson, B. J. (2015). A mex3 homolog is required for differentiation during planarian stem cell lineage development. *eLife* **4**, e07025.